Russian Journal of General Chemistry, Vol. 71, No. 7, 2001, pp. 1058–1065. Translated from Zhurnal Obshchei Khimii, Vol. 71, No. 7, 2001, pp. 1124–1131.

Complex Formation of Magnesium(II) with Octaaryltetraazaporphyrins in Pyridine

O. G. Khelevina, S. V. Rumyantseva, E. V. Antina, and N. Sh. Lebedeva

Ivanovo State University of Chemical Engineering, Ivanovo, Russia
Institute of Solution Chemistry, Russian Academy of Sciences, Ivanovo, Russia

Received December 14, 1999

Abstract — Complex formation of magnesium with octaphenyltetraazaporphyrin, octakis[*p*-(chloromethyl)-phenyl]tetraazaporphyrin, and octakis[*p*-(dodecylsulfamoyl)phenyl]tetraazaporphyrin from corresponding ligands and magnesium acetate in pyridine and pyridine–diethylamine was studied. Increase in the basicity of the medium favors a much faster reaction. Some suggestions concerning the mechanism of the reaction were made.

Tetraazaporphyrins react with metal salts, forming complexes according to Eq. (1) [1, 2].

$$H_2TAP + [MX_2(Solv)_{n-2}] \longrightarrow (Solv)_mMTAP + 2HX + (n - 2 - m)Solv. \quad (1)$$

Here H_2TAP is tetraazaporphyrin ligand, MTAP is metal complex of the tetraazaporphyrin, Solv is solvent, $[MX_2(Solv)_{n-2}]$ is solvation complex of the metal salt. Depending on the metal nature, solvent molecules may remain bound with the central metal atom as extra ligands.

Complex formation of metal acetates with tetraazaporphyrines in pyridine most frequently occurs by the bimolecular mechanism $S_{NE}2$ [3]. Pyridine molecules in the stage of activation of the system H_2TAP–salt effect solvation of endocyclic protons and force them out of the macroring plane. The reaction center acquires additional charge and thus gets more delocalized. The metal cation favors this process. Bond formation between the cation and tertiary nitrogen atoms of H_2TAP almost compensates for the energy consumption for M–Solv bond cleavage [scheme (2)].

Proceeding with our works [4–6], we have studied complex formation between octaaryltetraazaporphyrins $[H_2TAP(C_6H_4R)_8]$ and Mg^{2+} ions in pyridine and pyridine–diethylamine.

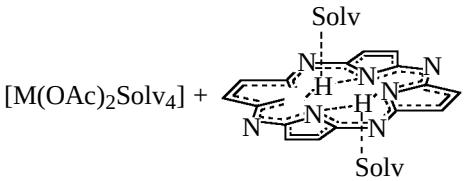

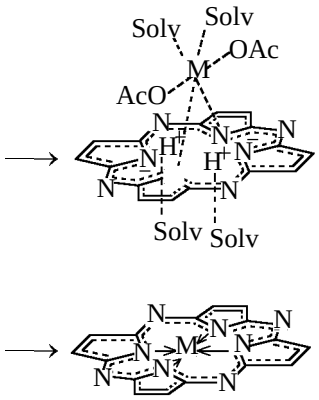

$$+ 2H^+_{Solv} + 2AcO^- + 4Solv. \quad (2)$$

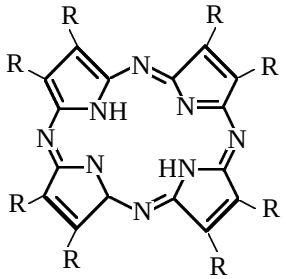

$H_2TAP(C_6H_4R)_8$

R = H, CH_2Cl, $SO_2NHC_{12}H_{25}$.

Complex formation of $H_2TAP(C_6H_4R)_8$ with magnesium acetate was performed with a large excess of the salt, i.e. under pseudo-first-order reaction conditions. Actually, the formation of $MgTAP(C_6H_4R)_8$

1070-3632/01/7107-1058 $25.00

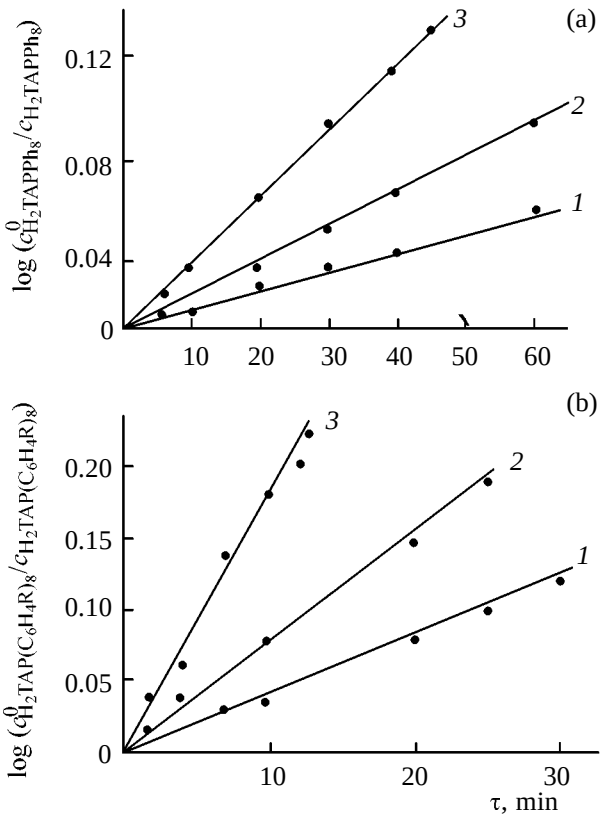

Fig. 1. Plot of $\log c^0_{H_2TAP(C_6H_4R)_8}/c_{H_2TAP(C_6H_4R)_8}$ vs. time for complex formation (a) of $H_2TAP(Ph)_8$ with $Mg(OAc)_2$ in pyridine–diethylamine at (*1*) 303, (*2*) 313, and (*3*) 323 K [$c_{Mg(OAc)_2}$ 1.36×10^{-3} M)] and (b) of $H_2TAP(C_6H_4SO_2NHC_{12}H_{25}$-*p*$)_8$ with $Mg(OAc)_2$ in pyridine at (*1*) 313, (*2*) 323, and (*3*) 333 K [$c_{Mg(OAc)_2}$ 0.89×10^{-3} M].

is a first-order reaction in $H_2TAP(C_6H_4R)_8$ concentration, which is evidenced by linear dependences of $\log (c^0_{H_2TAP(C_6H_4R)_8}/c_{H_2TAP(C_6H_4R)_8})$ on reaction time τ (Fig. 1). Therefore, the apparent and true rate constants can be calculated by Eqs. (3) and (4):

$$dc_{MgTAP(C_6H_4R)_8}/d\tau = k_{app}\, c_{H_2TAP(C_6H_4R)8}, \quad (3)$$

$$k_{app} = k\, c^n_{Mg(OAc)_2}. \quad (4)$$

Here k_{app} is the apparent rate constant, k is the true rate constant, and n is the reaction order in magnesium acetate.

Tables 1 and 2 list the kinetic parameters of complex formation of octaaryltetraazaporphyrins with magnesium acetate in pyridine and pyridine–diethylamine.

The experimental data showed that the rate constants of Mg–octaphenyltetraazaporphyrin and Mg–octakis[*p*-(dodecylsulfamoyl)phenyl]tetraazaporphyrin formation are almost independent on salt concentration. Figure 2 depicts the $\log k_{app}$–$\log c_{Mg(OAc)_2}$ dependences for complex formation of octaphenyltetraazaporphyrin and octakis[*p*-(dodecylsulfamoyl)-phenyl]tetraazaporphyrin in pyridine–diethylamine and pyridine, respectively. The reaction order in

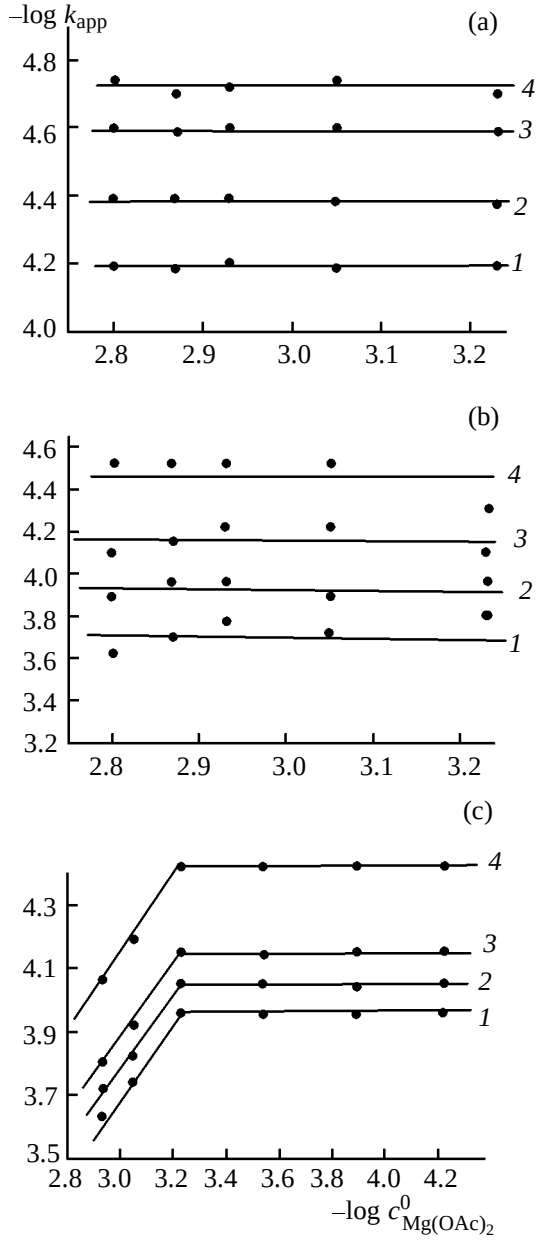

Fig. 2. Plot of $\log k_{app}$ vs. $\log c^0_{Mg(OAc)_2}$) for complex formation (a) with $H_2TAP(Ph)_8$ in pyridine–diethylamine at (*1*) 323, (*2*) 313, (*3*) 303, and (*4*) 298 K; (b) with $H_2TAP(C_6H_4SO_2NHC_{12}H_{25}$-*p*$)_8$ in pyridine at (*1*) 333, (*2*) 323, (*3*) 313, and (*4*) 298 K); and (c) with $H_2TAP(C_6H_4CH_2Cl$-*p*$)_8$ in pyridine at (*1*) 343, (*2*) 333, (*3*) 323, and (*4*) 298 K.

Table 1. Kinetic parameters of Mg–octaaryltetraazaporphyrin formation ($c^0_{Mg(OAc)_2}$ 0.89×10^{-3} M)

Compound	T, K	$k_{app} \times 10^4$, s^{-1}	E, kJ/mol	$\Delta S^{\neq}$, J mol^{-1} K^{-1}
	Pyridine–diethylamine (c_{NHEt_2} 1.36 M)			
$H_2TAP(Ph)_8$	298	0.19[a]	39 ± 2	–216 ± 5
(c_0 1.23×10^{-5} M)	303	0.25 ± 0.02		
	313	0.42 ± 0.05		
	323	0.66 ± 0.03		
	Pyridine			
$H_2TAP(Ph)_8$	298	1.00×10^{-2}[a]	71 ± 3	–130 ± 6
(c_0 1.23×10^{-5} M)	333	0.20 ± 0.05		
	343	0.44 ± 0.05		
	353	0.85 ± 0.06		
$H_2TAP(C_6H_4SO_2NHC_{12}H_{23}\text{-}n)_8$	298	0.26[a]	49 ± 2	–193 ± 7
(c_0 1.27×10^{-5} M)	313	0.61 ± 0.02		
	323	1.30 ± 0.03		
	333	1.92 ± 0.02		

[a] Calculated by the Arrhenius equation.

Table 2. Kinetic parameters of Mg–octakis[*p*-(chloromethyl)phenyl]tetraazaporphyrin formation in pyridine ($c^0_{H_2TAP(C_6H_4CH_2Cl\text{-}n)_8}$ 0.524×10^{-4} M)

$c_{Mg(OAc)_2}$, M	T, K	$k_{app} \times 10^3$, s^{-1}	E, kJ/mol	$\Delta S^{\neq}$, J mol^{-1} K^{-1}
6×10^{-5}	298	0.038[a]	20 ± 4	–272 ± 7
	323	0.071 ± 0.002		
	333	0.090 ± 0.004		
	343	0.112 ± 0.004		
1.3×10^{-4}	298	0.038[a]	20 ± 4	–272 ± 7
	323	0.070 ± 0.001		
	333	0.091 ± 0.005		
	343	0.110 ± 0.004		
2.9×10^{-4}	298	0.038[a]	21 ± 4	–272 ± 6
	323	0.073 ± 0.002		
	333	0.090 ± 0.005		
	343	0.112 ± 0.004		
5.9×10^{-4}	298	0.038[a]	20 ± 3	–272 ± 8
	323	0.07 ± 0.002		
	333	0.09 ± 0.006		
	343	0.11 ± 0.004		
8.9×10^{-4}	298	0.065[a]	19 ± 1	–268 ± 4
	323	0.121 ± 0.004		
	333	0.152 ± 0.004		
	343	0.180 ± 0.005		
1.18×10^{-3}	298	0.087[a]	17 ± 1	–265 ± 4
	323	0.160 ± 0.002		
	333	0.191 ± 0.004		
	343	0.233 ± 0.004		

[a] Calculated by the Arrhenius equation.

magnesium acetate *n*, measured by the slope ratios of the above dependences, proved to be zero. Apparently, with these porphyrins, the limiting stage of the complex formation with Mg occurs by a mechanism similar to that established for complex formation of octaphenyltetraazaporphyrin with Zn^{2+}, Cu^{2+}, Cd^{2+}, Co^{2+}, and Ni^{2+} in pyridine [7]. According to this mechanism, coordination in tetraazaporphyrins can involve both internal and external *meso*-nitrogen atoms to form with metal acetate unstable intermediate complexes of the amine type [Eq. (5)]:

$$H_2TAP(C_6H_4R)_8 + [M(OAc)_{2Solv_4}] \rightleftarrows H_2TAP(C_6H_4R)_8[M(OAc)_{2Solv_3}] + Solv. \quad (5)$$

Such intermediate complexes can convert into $MTAP(C_6H_4R)_8$ via migration of the metal cation from the *meso*-nitrogen atom to the reaction center [scheme (6)]:

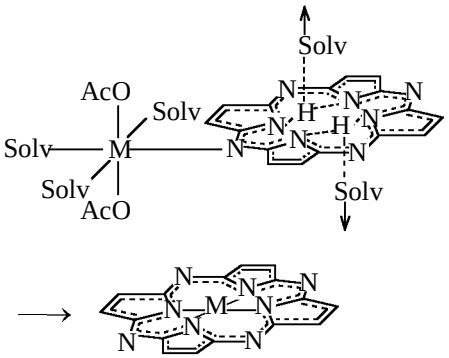

$$+ 2H^+_{Solv} + 2AcO^- + 3Solv. \quad (6)$$

Probably, the intermediate amine complex is formed not only by donor–acceptor interaction, but also by hydrophobic ππ interaction between $H_2TAP(C_6H_4R)_8$ and ligand environment of the metal. Such interaction of *meso*-nitrogen atoms with metal cations has been found in the Ni(II) complex of tetrakis(*S*,*S*-dibutyltin)–octathiolatotetraazaporphyrin [8]. The formation of the amine complex is favored by electron-donor substituents in pyrrole rings of the tetraazaporphyrin macroring, which increase the electron density on the *meso*-nirogen atoms [3], as well as by strong solvation of the reaction center, which hinders axial attack by the metal [3].

The stability constants of first acidic forms (protonated by *meso*-nitrogens) of octaphenyltetraazaporphyrin and tetraazaporphyrin (pK_1 1 and 0.15, respectively) show that phenyl radicals actually increase the basicity of the macroring by increasing the electron density on *meso*-nitrogen atoms by the +*I* effect [9].

The strong solvation of the reaction center in octaphenyltetraazaporphyrin by pyridine is confirmed by the following fact: The splitting of the *Q* band in the electronic absorption spectrum of octaphenyltetraazaporphyrin in pyridine is 80 cm^{-1} smaller than in the spectrum in chlorobenzene (solvatochromic effect). On prolonged standing of the pyridine solution of octaphenyltetraazaporphyrin at room temperature or on its boiling for some hours a "pyridinium salt" or an acid–base complex [Eq. (7)] are formed [7].

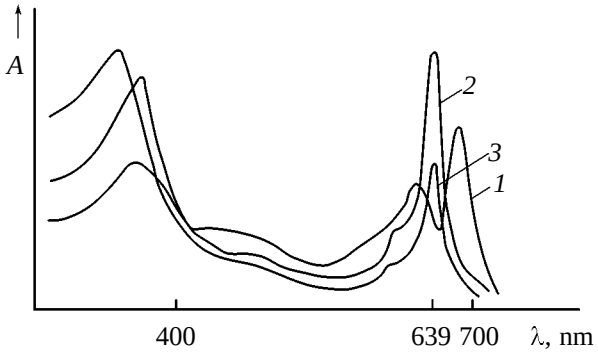

Fig. 3. Electronic absorption spectra in pyridine of (*1*) $H_2TAP(Ph)_8$ (freshly prepared solution), (*2*) $MgTAP(Ph)_8$, and (*3*) "pyridinium salt" of $H_2TAP(Ph)_8$.

$$H_2TAP(Ph)_8 + 2PyH \rightleftarrows 2(PyH_2^+)\cdots TAP(Ph)_8^{2-}. \quad (7)$$

This reaction has first been observed by Whalley [10] for tetraazaporphyrin, its alkyl derivatives, and phthalocyanine. The referee showed that such complexes with the mentioned tetraazaporphyrins can form only photochemically. With more acidic tetraazaporphyrins (tetrabromotetraazaporphyrin, tetrachlorotetraazaporphyrin), the formation of the "pyridinium salt" in pyridine is complete at room temperature within 40–60 min [11]. The changes in the electronic absorption spectra of tetraazaporphyrins, that accompany acid–base complex formation, are similar to those observed on addition of metal ions, implying removal of protons from the reaction center with increase in the ligand symmetry from D_{2h} to D_{4h} (Fig. 3). Studies on acid–base interactions of tetraazaporphyrins with various bases in chlorobenzene showed that the complexes formed differ in the degree of charge transfer from the tetraazaporphyrin to the donor center of the base, which depends on the electronic and geometric structure of the tetraazaporphyrin and base, as well as on the features of solvation of the resulting acid–base forms [12] [scheme (8)].

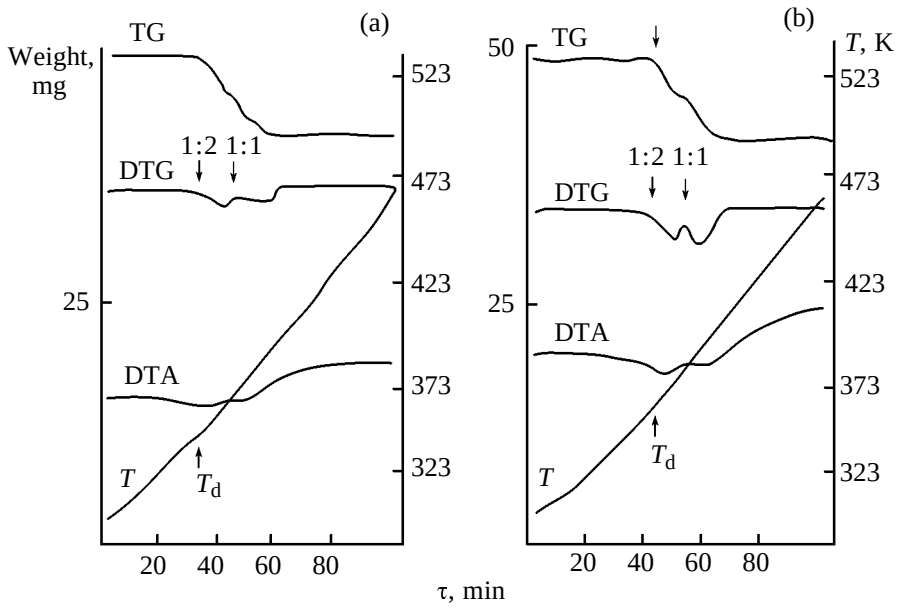

Fig. 4. Thermoanalytical curves for the crystal solvates (a) of $H_2TAP(Ph)_8$ with pyridine and (b) of $MgTAP(Ph)_8$ with pyridine.

$$H_2TAP + B \rightleftarrows \underset{\text{H complex}}{B\cdots H\cdots TAP\cdots H\cdots B} \rightleftarrows \underset{\text{ion–ion associate}}{B\cdots H\cdots TAP^{-}\cdots H^{+}B} \rightleftarrows \underset{\text{ion–ion associate}}{BH^{+}\cdots TAP^{2-}\cdots H^{+}B} \rightleftarrows \underset{\text{solvent-separated ion pair}}{TAP^{2-}//2BH^{+}} \rightleftarrows \underset{\text{dianion}}{TAP^{2-}} + 2BH^{+}. \quad (8)$$

The high thermal stability of octaphenyltetraazaporphyrin allowed us to perform a thermogravimetric investigation of the crystal solvate of octaphenyltetraazaporphyrin with pyridine in the range 15–150°C, where decomposition of the compound is excluded. Analysis of the thermoanalytical curve (Fig. 4) shows that octaphenyltetraazaporphyrin forms with pyridine an $H_2TAP(Ph)_8$–2 PyH complex which is stable in crystal solvate up to 68°C. The enthalpy of the decomposition of the complex, accompanied by evolution of gaseous pyridine, was estimated (ΔH 41.2 ± 0.4 kJ/mol). The low acidity of octaphenyltetraazaporphyrin (pK_{a1} 13.79 in DMF [9]), the low dielectric constant of pyridine (ε 12.3 [13]), as well as the energetic characteristics and the composition of the complex suggest that the "pyridinium salt" of octaphenyltetraazaporphyrin is an H complex like $[HPy\cdots H\cdots TAP(Ph)_8\cdots H\cdots PyH]$ [12] whose bonds are close in nature to donor–acceptor bonds, as evidenced by the ΔH value. The "pyridinium salt" of octaphenyltetraazaporphyrin is insusceptible to complex formation, since its reaction center is blocked by pyridine molecules.

In the binary mixture pyridine–diethylamine the Mg–octaphenyltetraazaporphyrin complex is formed 20 times faster than in pyridine (Table 1). Diethylamine, being a stronger base than pyridine, accelerates the reaction by enhancing polarization of N–H bonds, which favors formation of the $TAP(Ph)_8^{2-}$ anion and thus the transition state of the reaction.

Earlier Stuzhin *et al.* [4] studied complex formation of magnesium with unsubstituted tetraazaporphyrin in pyridine. Comparison of the rate constants of complex formation of tetraazaporphyrin and octaphenyltetraazaporphyrin in pyridine showed that octaphenyltetraazaporphyrin coordinates with Mg ions 2 orders of magnitude faster than tetraazaporphyrin (k_{app}^{298} 10^{-6} and 9.6×10^{-9} s^{-1}, respectively, at $c^0_{Mg(OAc)_2}$ 3×10^{-4} M). It is known [3] that the rate of coordination of tetraazaporphyrins with metal ions in basic solvents is controlled by N–H bond cleavage, and electron-donor substituents (such as phenyl) should decelerate the reaction. This is the case in complex formation of octaphenyltetraazaporphyrin with Cu^{2+}, Co^{2+}, Zn^{2+}, Cd^{2+}, and Ni^{2+} ions [3]. The first coordination sphere of Mg^{2+} in pyridine is unlike the coordination spheres of transition metal ions and is formed by six pyridine molecules, and anions reside in the second coordination sphere: $[Mg(PyH)_6](OAc)_2$ [4]. This is the reason why tetraazaporphine coordinates with Mg(II) slower by a factor of 10^5 than with Zn(II) or Cd(II). The higher rate of coordination of octaphenyltetraazaporphyrin with Mg(II) can be explained by that the reaction here occurs by a mono-

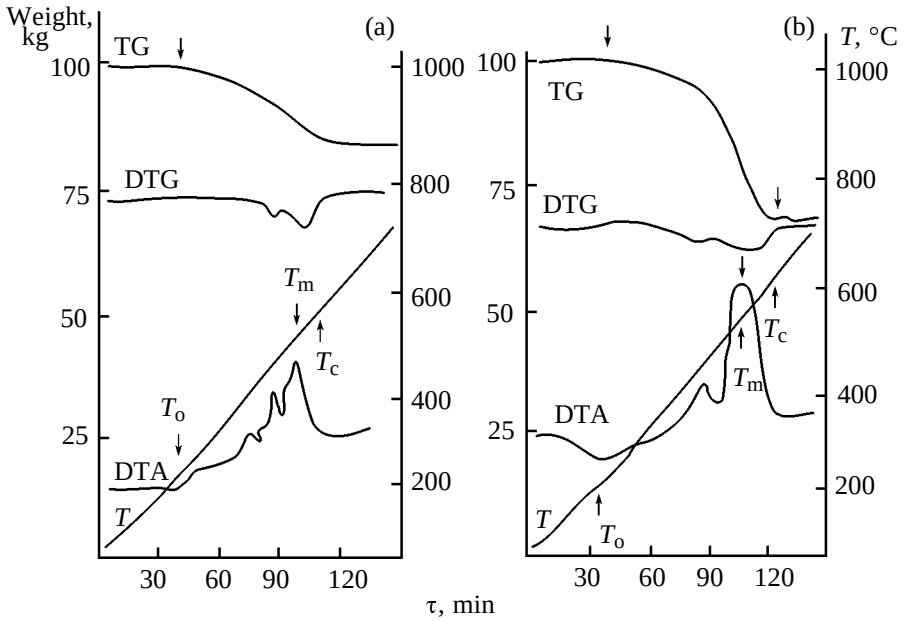

Fig. 5. Thermoanalytical curves of thermooxidative decomposition of (a) H_2TAP(Ph) and (b) MgTAP(Ph)$_8$.

molecular mechanism, where the solvation shell of Mg^{2+} in the intermediate anionic complex is already strongly rearranged and thus weaker affects the limiting stage of the reaction.

Introduction in phenyl radicals of octaphenyltetraazaporphyrin of the electron–acceptor dodecylsulfamoyl groups reduces the electron density on *meso*-nitrogen atoms and thus unfavors the monomolecular limiting stage. However, this mechanism is still operative with the sulfamoyl derivative, probably, because of the strong solvation of the reaction center; therewith, autosolvation may occur due to the presence of $C_{12}H_{25}$ groups (formation of quasi-solvation shells). The same effect has been observed with the Zn–bis(octadecylamino)methyltetrabenzoporphine complex formation [14]. The rate constants of complex formation of the sulfamoyl derivative with magnesium acetate is much higher than the corresponding values for octaphenyltetraazaporphine; therewith, the activation energy and entropy are reduced by almost half. Such a reduced activation energy suggests stronger solvation of the reaction center of the sulfamoyl derivative in the transition state.

The complex formation of octakis[*p*-(chloromethyl)phenyl]tetraazaporphyrin in pyridine occurs by a more complicated mechanism (Table 2). At the concentrations of $Mg(OAc)_2$ from 6×10^{-5} to 5.9×10^{-4} M the reaction order in magnesium acetate is zero, and at the concentrations 8.9×10^{-4} and 1.18×10^{-3} M it is 0.7. Probably, at higher salt concentrations the intermediate amine complex formed by *meso*-nitrogen atom, reacts with magnesium acetate by a bimolecular mechanism, like with Mg–tetraazaporphyrin complex formation [4] (Fig. 2).

The above results allowed us to rank the octaaryl–tetraazaporphyrins studied by their reactivity toward magnesium acetate in pyridine as follows: $H_2TAP(Ph)_8$ < $H_2TAP(C_6H_4CH_2Cl\text{-}p)_8$ < $H_2TAP(C_6H_4SO_2NHC_{12}H_{25}\text{-}p)_8$.

We performed a thermogravimetric study of thermooxidative decomposition of octaphenyltetraazaporphyrin and its magnesium complex (Fig. 5). The process of thermooxidative decomposition of octaphenyltetraazaporphyrin begins at 220°C and completes at 550°C, and it is accompanied by exothemic effects (DTA, the maximum exothermic effect is observed at 505°C) and a full weight loss at the end of the process. Compared with the ligand, the magnesium complex is less stable thermally (the respective temperatures for the ligand are 200, 600, and 530°C), which is consistent with the regularities reported for porphyrin ligands and complexes [15]. It should be noted that octaphenyltetraazaporphyrin and Mg–octaphenyltetra–azaporphyrin are less stable thermally than previously studied porphyrins and porphyrin complexes, which may be due to the peculiar molecular and crystal structure of the former and effects of the phenyl substituents.

The thermogravimetric analysis of the crystal solvate of Mg–octaphenyltetraazaporphyrin with pyridine, like of the crystal solvate of the ligand, was performed in the range 15–150°C. The thermoanalytical curve

shows (Fig. 4) that the magnesium complex forms with pyridine an extra complex of the composition $MgTAP(Ph)_8$–2PyH which is stable in crystal solvate up to 86°C (ΔH 53.2 ± 0.3 kJ/mol). The presence in the crystal solvate of the energetically stable complex $MgTAP(Ph)_8 \cdot 2PyH$ gives us grounds to propose that in pyridine, too, Mg(II) in the Mg complex takes up in the course of complex formation two pyridine molecules as extra ligands. Analogous data on the composition of pyridine extra complexes have been obtained for other magnesium(II) porphyrins [16].

EXPERIMENTAL

Octaphenyltetraazaporphyrin and octakis[*p*-(chloromethyl)phenyl]tetraazaporphyrin were obtained by the procedures in [17] and [18], respectively. Pyridine and diethylamine were purified and dried by the procedures in [19]. Magnesium acetate of chemical grade was recrystallized from glacial acetic acid.

Kinetic measurements were performed in a temperature-controlled cell of a Specord M-40 spectrophotometer, where we placed solutions of octaarylporphyrine and magnesium acetate of specified concentrations and at a specified temperature and measured in certain intervals the optical densities of the solutions at the absorption maxima of the resulting complexes {637 nm for Mg–octaphenyltetraazaporphyrin, 642 nm for Mg–octakis[*p*-(dodecylsulfamoyl)phenyl]-tetraazaporphyrine, and 646 nm for Mg–octakis[*p*-(chloromethyl)phenyl]tetraazaporphyrin}. The current and final concentrations of octaaryltetraazaporphyrines were determined by Eq. (9):

$$c = c_0(A_\tau - A_\infty)/(A_0 - A_\infty). \quad (9)$$

Here A_0, A_τ, and A_∞ are the optical densities at the beginning of the reaction, at time τ, and at the end of the reaction; c_0 and c are the initial and current concentrations of tetraazaporphyrin.

Thermal analysis was performed on a MOM-1 000D derivatograph (Hungary). Before analysis the compounds were dried to constant weight at 25–100°C. Crystal solvates were prepared by a procedure similar to that described in [20] and involving slow crystallization from concentrated solutions at 25–40°C. To remove weakly bound solvent molecules, the crystal solvate was dried in a vacuum to constant weight (25–50°C). The samples were 30–40 (tetraazaporphyrines and complexes) or 10–25 mg (crystal solvates). The heating rate in the analysis of crystal solvates in nonisothermal conditions was 0.6 deg/min. The heating rate in thermal decomposition studies was 5 deg/min. The decomposition temperatures T_d of porphyrins were determined from the slopes of the TG curves [21] and additionally checked by the electronic absoption spectra of samples taken below and above that temperature. The physicochemical characteristics of the molecular complexes of porphyrins with pyridine were determined from the thermogravimetric data, according to [22]. The reproducibility of the thermoanalytical curves was controlled by five runs with freshly prepared samples.

ACKNOWLEDGMENTS

The authors are grateful to V.P. Kulinich and S.I. Vasil'ev for supplying the sample of octakis[*p*-(dodecylsulfamoyl)phenyl]tetraazaporphyrin.

REFERENCES

1. Berezin, B.D., *Koordinatsionnye soedineniya porfirinov i ftalotsianina* (Coordination Compounds of Porphyrins and Phthalocyanine), Moscow: Nauka, 1978.
2. Stuzhin, R.A. and Khelevina, O.G., *Coord. Chem. Rev.*, 1996, vol. 147, no. 1, pp. 41–86.
3. *Uspekhi khimii porphyrinov* (Advances in Pophyrin Chemistry), Golubchikov, O.A., Ed., St. Petersburg: St. Petersb. Gos. Univ., 1997, pp. 150–202.
4. Stuzhin, P.A., Khelevina, O.G., and Berezin, B.D., *Zh. Fiz. Khim.*, 1987, vol. 61, no. 1, pp. 82–85.
5. Khelevina, O.G. and Rumyantseva, S.V., *Koord. Khim.*, 1999, vol. 25, no. 4, pp. 261–264.
6. Khelevina, O.G. and Rumyantseva, S.V., *Koord. Khim.*, 1999, vol. 25, no. 5, pp. 330–333.
7. Berezin, B.D, Khelevina, O.G., Gerasimova, N.D., and Stuzhin, P.A., *Zh. Fiz. Khim.*, 1982, vol. 56, no. 11, pp. 2768–2772.
8. Velazques, C.S., Broderick, W.E., Sabat, M., Barret, A.G.M., and Hoffman, B.M., *J. Am. Chem. Soc.*, 1990, vol. 112, no. 20, pp. 7408–7410.
9. *Phthalocyanines: Properties and Applications*, Leznoff, C.C. and Lever, A.B.P., Eds., New York: VCH, 1996, vol. 4, pp. 19–77.
10. Whalley, M.J., *J. Chem. Soc.*, 1961, no. 3, pp. 866–869.
11. Khelevina, O.G., Chizhova, N.V., and Berezin, B.D., *Koord. Khim.*, 1991, vol. 17, no. 3, pp. 400–404.
12. Khelevina, O.G. and Petrov, O.A., *Koord. Khim.*, 1997, vol. 23, no. 11, pp. 803–811.
13. Bureiko, S.F. and Oktyabr'skii, V.P., *Kinet. Katal.*, 1986, vol. 27, no. 3, pp. 565–569.
14. *Kompleksoobrazovanie v nevodnykh rastvorakh* (Complex Formation in Nonaqueous Solutions), Kres-

tov, G.A., Ed., Moscow: Nauka, 1989, p. 217.

15. Lebedeva, N.Sh., Antina, E.V., Berezin, M.B., Semeikin, A.S., and Bukushina, G.B., *Zh. Fiz. Khim.*, 2000, vol. 74, no. 7, pp. 1141–1146.
16. Miller, J.R. and Dorough, G.D., *J. Am. Chem. Soc.*, 1952, vol. 7, no. 16, pp. 3977–3981.
17. Cook, A.H. and Linsted, R.P., *J. Chem. Soc.*, 1937, no. 4, pp. 929–934.
18. Petrova, R.A., Khelevina, O.G., Berezin, B.D., and Saidelova, F.L., *Izv. Vyssh. Uchebn. Zaved. Khim. Khim. Tekhnol.*, 1993, vol. 36, no. 2, pp. 102–106.
19. *Organikum: organisch-chemisches Grundpraktikum*, Berlin: Wissenschaften, 1976, 15 ed. Translated under the title *Organikum: praktikum po organicheskoi khimii*, Moscow: Mir, 1979, vol. 2.
20. Kirner, I.F., Reed, C.A., and Scheidt, W.R., *J. Am. Chem. Soc.*, 1977, vol. 99, no. 4, pp. 1093–1101.
21. Badea, M., Marinescu, D., and Segal, E., *Thermochim. Acta*, 1989, vol. 149, no. 1, p. 198.
22. Antina, E.B., Barannikov, V.P., V'yugin, A.I., Nikiforov, M.Yu., and Krestov, G.A., *Zh. Neorg. Khim.*, 1990, vol. 35, no. 2, pp. 400–404.